Tetrahedron 70 (2014) 3306–3313

Contents lists available at ScienceDirect

Tetrahedron

journal homepage: www.elsevier.com/locate/tet

Task-specific ionic liquid incorporating anionic heteropolyacid-catalyzed Hantzsch and Mannich multicomponent reactions. Ionic liquid effect probed by ESI-MS(/MS)

Haline G.O. Alvim[a], Giovana A. Bataglion[b], Luciana M. Ramos[a], Aline L. de Oliveira[a], Heibbe C.B. de Oliveira[a], Marcos N. Eberlin[b], Julio L. de Macedo[c], Wender A. da Silva[d,*], Brenno A.D. Neto[a,*]

[a] *Laboratory of Medicinal and Technological Chemistry, University of Brasilia (IQ-UnB), Campus Universitario Darcy Ribeiro, CEP 70904970, P.O. Box 4478, Brasilia-DF, Brazil*
[b] *ThoMSon Mass Spectrometry Laboratory, University of Campinas-UNICAMP, Campinas SP 13085-970, Brazil*
[c] *Laboratory of Catalysis, Institute of Chemistry, University of Brasília, P.O. Box 4478, CEP 70904970 Brasília, DF, Brasil*
[d] *Laboratory for Bioactive Compounds Synthesis, University of Brasilia (IQ-UnB), Campus Universitario Darcy Ribeiro, CEP 70904970, P.O. Box 4478, Brasilia-DF, Brazil*

ARTICLE INFO

Article history:
Received 21 August 2013
Received in revised form 7 October 2013
Accepted 11 October 2013
Available online 18 October 2013

Keywords:
Ionic liquids
Multicomponent reactions
Mechanism
ESI-MS
Bioactive

ABSTRACT

A task-specific ionic liquid with a Bronsted acid (1-(3-sulfopropyl)-3-methylimidazolium hydrogen sulfate, namely **MSI**) bearing an anionic heteropolyacid derivative ($[PW_{12}O_{40}]^{3-}$, namely **PW**) were used as an efficient catalyst for the three-component Mannich and Hantzsch reactions. Using **(MSI)$_3$PW** as the catalyst supported in imidazolium-based ionic liquids allowed these multicomponent reactions to take place in good to excellent yields. The Mannich reaction, performed at room temperature, was also evaluated by means of electrospray (tandem) mass spectrometry—ESI-MS(/MS). ESI-MS data pointed to the origin of the ionic liquid effect, i.e., formation of ion pairs with the charged reaction intermediates and furthers association into larger supramolecular aggregates. DFT calculations revealed the strength of the supramolecular interactions between the charged species detected by ESI-MS and the spontaneity association of these ion pairs affording larger supramolecular aggregates.

1. Introduction

Multicomponent reactions (MCR) are useful tools in organic synthesis[1–3] giving direct, elegant, and simple access to bioactive compounds libraries.[4–6] Multi-reagents brought together in a one-pot version is a very attractive protocol, especially from the viewpoint of eco-friendly and sustainable conditions,[7] but still suffers from many drawbacks, as already reviewed.[8–10] Long reaction times, harsh reaction conditions, reagents excesses, high temperatures, toxic solvents, expensive catalysts, demanding purification, and low yields are major limitations of MCR. Catalysis occupies therefore a central role toward the development of more environmentally-friend and efficient MCR conditions aiming at better yields, selectivities, and atom economy;[11–15] i.e. highly desired features for green chemistry progress.

Ionic liquids (IL), especially those based on the imidazolium cation[16–18] (Fig. 1), have been applied as supporters for catalysts and/or as reaction media for many organic transformations that are difficult to occur or are inefficient in classical organic solvents.[19–21] IL are, definitely, a major class of exceptional ionic fluids used as solvents for synthesis and catalysis.[22–24] IL are already successfully used in the chemical industry[25] and a likely possible way to environmental acceptability.[26]

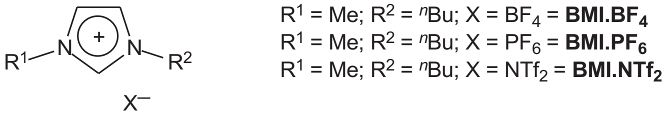

Fig. 1. 1,3-Dialkylimidazolium-based ionic liquids commonly used in homogeneous or heterogeneous catalysis.

The combination of MCR with IL (for catalyzed reactions) has been regarded as ‘a perfect synergy for eco-compatible heterocyclic synthesis’, as ‘a promising strategy for the development of valuable eco-

---

* Corresponding authors. Tel.: +55 61 31073867; fax: +55 61 31073901 (B.A.D.N.); tel.: +55 61 31073860 (W.A.S.); e-mail addresses: wender@unb.br (W.A. da Silva), brenno.ipi@gmail.com (B.A.D. Neto).

0040-4020/$ – see front matter © 2013 Elsevier Ltd. All rights reserved.
http://dx.doi.org/10.1016/j.tet.2013.10.033

compatible organic synthesis procedures' and, finally, as 'an excellent media for multiple bond-forming transformations'.[27] IL have already proved to be outstanding media for MCR.[27–29] The promising combination of MCR and IL (catalyzed reactions) is just beginning to be explored and still there are much to be achieved. Task-specific ionic liquids (TSIL) have also been successfully employed as alternative acid[30] and basic[31] catalysts to perform MCR. Since it is possible to diversely functionalize the anion or the cation (or both) to tailor a TSIL, it is reasonable to envisage specific interactions and properties aiming at improved catalytic conditions due to the presence of those tags tethered to the structure of the catalyst.[32–35]

Considering the likely advantages of using IL (and/or TSIL) under catalytic conditions to promote MCR, we have demonstrated the synergic effect of a copper (pre)catalyst and the anionic moiety of BMI·PF_6 to the formation and stabilization of key reactive intermediates in the multicomponent Biginelli reaction.[36] In another recent study, we successfully tested a new iron-containing TSIL as a catalyst of dual activation mode to obtain a library of bioactive dihydropyrimidinones from an MCR.[37] More recently, we have analyzed and compared the use of a TSIL incorporating anionic heteropolyacid derivative (Scheme 1) as the catalyst for the three-component Biginelli reaction under homogeneous (Scheme 1) and heterogeneous conditions.[38]

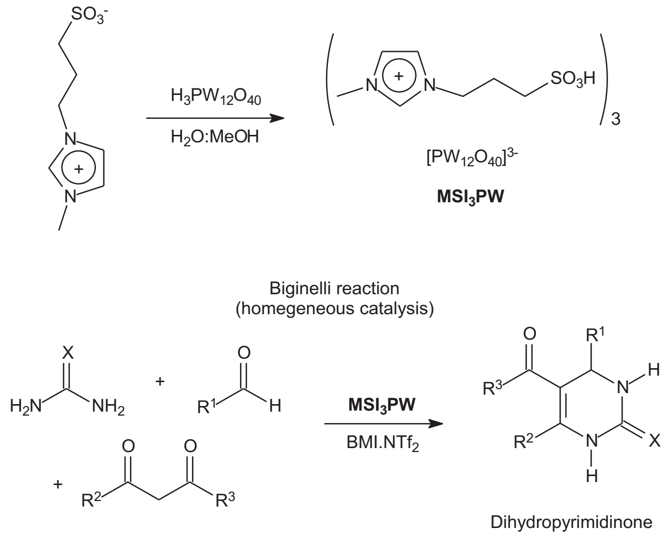

Scheme 1. Synthesis of the Bronsted acid task-specific ionic liquid (**MSI** cation) with anionic heteropolyacid derivative ($[PW_{12}O_{40}]^{3-}$, **PW** anion) applied as the catalyst (**MSI$_3$PW**) for the Biginelli reaction.[38]

In the example depicted in Scheme 1,[38] equimolar quantities of the three components could be used. The catalyst also showed to be highly active in BMI·NTf_2, whereas those reactions carried out in BMI·BF_4 or BMI·PF_6 lead to reagent decomposition and lower yields. Under the best developed condition, the Biginelli adduct could be obtained in quantitative yields in just a few hours and the system could be recycled. Due to our interest in MCR and catalytic reactions conducted in IL,[39–41] we investigate the use of **MSI$_3$PW** for Hantzsch and Mannich MCR and report herein that it function as a very active catalyst with impressive IL effect. We also evaluated the IL effect, via ion-pairing and larger supramolecular aggregates, by electrospray ionization (tandem) mass spectrometry ESI-MS(/MS) and DFT calculations.

2. Results and discussion

The three-component Hantzsch and Mannich reactions (Scheme 2) were conducted using **MSI$_3$PW** as the catalyst in BMI·NTf_2. **MSI$_3$PW** was synthesized and characterized as described elsewhere.[38,42] Briefly, the zwitterionic species (see Scheme 1) is treated with $H_3PW_{12}O_{40}$ (HPW—phosphotungstic acid) affording the desired catalyst in quantitative yields with the heteropolyacid derivative as the counteranion ($[PW_{12}O_{40}]^{3-} \equiv PW^{3-}$, namely herein as **PW**).

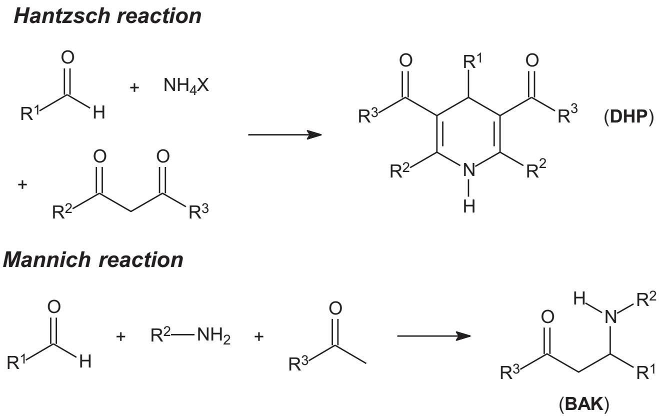

Scheme 2. Hantzsch and Mannich three-component reactions performed using **MSI$_3$PW** as the catalyst under homogeneous conditions and BMI·NTf_2 as the ionic media.

Aiming at the synthesis of some 1,4-dihydropyridines (**DHP**), we initially tested the Hantzsch[43–45] reaction applying the best catalytic conditions previously developed for MCR using **MSI$_3$PW** as the catalyst,[38] i.e., 90 °C, 4 h of reaction and 5 mol % of the catalyst supported in BMI·NTf_2. **DHP** has been found to exhibit beneficial biological effects, such as that for cardiovascular diseases acting as calcium channel blockers.[46] The Hantzsch reaction catalyzed by **MSI$_3$PW** yielded **DHP** in good to excellent yields (Table 1). Ammonium acetate may be replaced by ammonium chloride but a slight overall reduction in yields (∼5–8%) was noted.

Table 1
Hantzsch reaction catalyzed by **MSI$_3$PW** (5 mol %) at 90 °C for 4 h in BMI·NTf_2 (homogeneous system)

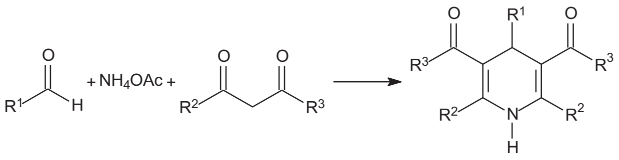

Entry	R^1	R^2	R^3	Yield (%)	DHP
1	Ph	CH_3	CH_3CH_2O	99	**DHP**(**a**)
2	3-OH–Ph	CH_3	CH_3CH_2O	87	**DHP**(**b**)
3	H	CH_3	CH_3CH_2O	84	**DHP**(**c**)
4	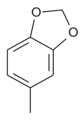	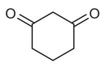		98	**DHP**(**d**)
5	Ph	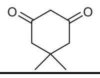		98	**DHP**(**e**)

Another advantage of our protocol was that no reagent excess was required to perform the Hantzsch MCR, and four bioactive **DHP**(**a–c**,**e**),[47–49] used as antioxidants, antimicrobial, anticoagulant, and channel blockers were directly synthesized in good to excellent yields (84–99%).

Having verified the excellent catalytic activity of **MSI_3PW**, we tested it to promote another three-component reaction, i.e., the Mannich reaction (Scheme 2), but now at conditions close to room temperature. Note that this reaction has been found to be very sensitive to temperature and Mannich[50–52] adducts (β-amino carbonyl compounds, **BAK**) are often thermo-unstable. Side reactions and decompositions of both reagents and products are normally favored with increased temperatures; therefore low temperatures are normally applied for this MCR.[53–55] More efficient Mannich reactions would be highly desirable since this MCR provides direct and simple access to β-amino carbonyls (Scheme 2), which are units found in many natural and synthetic products of pronounced biological activities.[56] All Mannich reactions (Table 2) were therefore conducted using equimolar quantities of the reagents at 30 °C.

Note in Table 2 that fortunately all Mannich products were synthesized in good to excellent yields (75–98%) at just 30 °C and again with no reagent excess. Some of the **BAK** showed to be highly unstable after isolation (see NMR spectra in the Supplementary data file to note the degradation), but unstable **BAK** can be isolated and immediately used as synthetic intermediates,[57–60] as reviewed elsewhere.[61]

Table 2
Mannich reaction catalyzed by **MSI_3PW** (5 mol %) at 30 °C in BMI·NTf_2

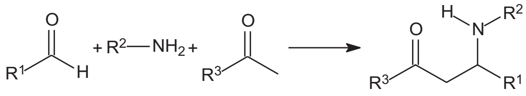

Entry	R^1	R^2	R^3	Yield (%)	BAK
1	Ph	Ph	Ph	95	**BAK(a)**
2	Ph	4-NH_2–Ph	Ph	85	**BAK(b)**
3	Ph	4-Ph–NO_2	Ph	98	**BAK(c)**
4	Ph	4-Ph–NH_2	4-OH–Ph	75	**BAK(d)**
5	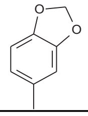	4-Ph–NO_2	Ph	80	**BAK(e)**

Since the Mannich reaction was efficiently performed under amenable conditions, we decided to investigate via ESI-MS(/MS) its mechanism as well as the IL effect over this MCR. ESI-MS is known for its efficient and accurate analysis of reaction solution components because of its capability of fast and sensitive 'fishing' of ionic reaction partners from solution directly to the gas phase as undisturbed 'cold' ions; therefore acting as a proper bridge connecting solution and gas phase chemistries.[62] Investigations of reaction mechanisms is one of the beauties of the Nobel laureate ESI-MS technique, which is capable of providing continuous snapshots of the reaction solution, hence allowing the online interception and characterization of reaction intermediates and of their appearance and fading[63–65] (including transient species[66]), hence the dynamic ionic changes[67] during the whole reaction time period.[68]

Initially, the **MSI_3PW** catalyst was characterized in both the positive and negative ion modes, i.e., via ESI(−)-MS and ESI(+)-MS. ESI(−)-MS (Fig. 2A) revealed the triply charged **PW^{3-}** as the most abundant ion (methanolic solution) followed by [**PW**+H]$^{2-}$. Note that no doubly protonated ion [**PW**+2H]$^{-}$ could be detected; therefore indicating proper dissociation of the Bronsted acid moiety. Interestingly, doubly charged ion [**PW**+**MSI**]$^{2-}$ was also detected due to the supramolecular association of **MSI** cation with **PW^{3-}** anion. This association of cations and anions (supramolecular) is common in the chemistry of IL and TSIL derivatives.[69] For ESI(+)-MS, only the TSIL cation **MSI** (m/z 205) could be detected and its ESI(+)-MS/MS was acquired (Fig. 2B).

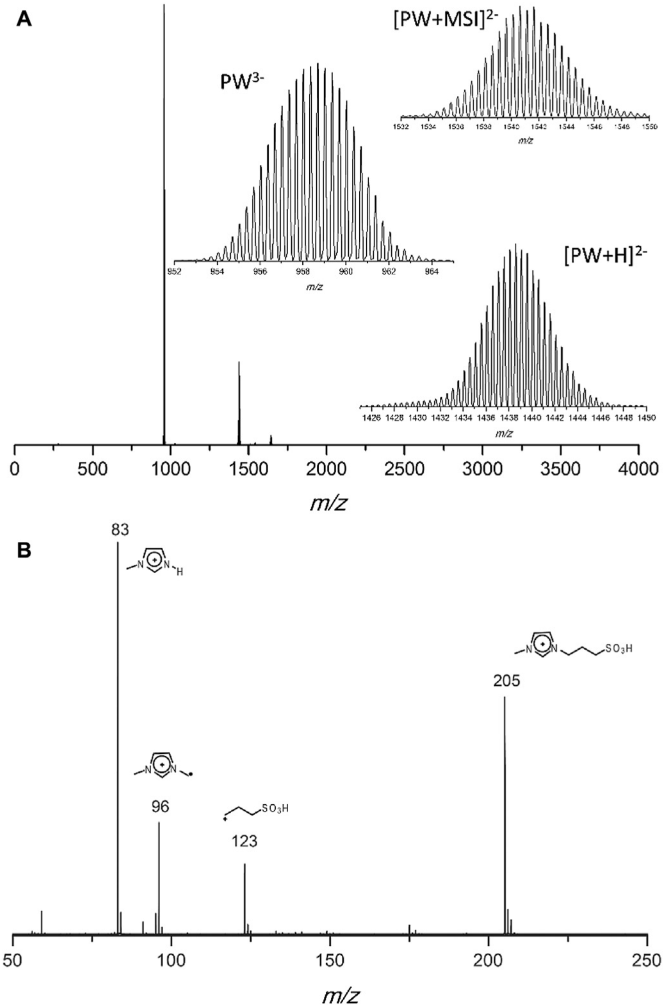

Fig. 2. (A) ESI(−)-MS of the methanolic solution of the **MSI_3PW** catalyst. **MSI** is the SO_3H functionalized imidazolium cation derivative (m/z 205) and **PW** is $[PW_{12}O_{40}]^{3-}$. (B) ESI(+)-MS/MS of the **MSI** cation.

After, the **MSI_3PW** catalyst was also subjected to ESI(−)-MS (Fig. 3) now in the presence of the IL (BMI·NTF_2).

Note in Fig. 3 that the [**PW**+**MSI**]$^{2-}$ anion could not be detected. Instead, the detection of [**PW**+BMI]$^{2-}$ anion revealed that in the presence of the IL, the cation BMI efficiently replaces the cation **MSI**. The ESI(−)-MS of Fig. 3 also shows the detection of the monoprotonated [**PW**+H]$^{2-}$ anion, but at a reduced abundance as compared to Fig. 2, in accordance with the expected acidic strength increase in the IL media. It has been already demonstrated that Bronsted acids (and Bronsted acids TSIL) can behave as superacids when supported (or embedded) in IL.[70,71] The ESI-MS data obtained for the **MSI_3PW** catalyst in the presence of BMI·NTf_2 is therefore in accordance with this predictable behavior, that is, [**PW**+H]$^{2-}$ had its abundance significantly diminished indicating the dissociation of the acid was even at a larger extent; i.e., a more effective acid strength of the catalyst because of both the additional interactions found in the ionic fluid and the consequent stabilizing effects associated with these supramolecular interactions.

After the catalyst characterization, we first monitored by ESI(+)-MS the Mannich reaction to investigate the possible intervention of the IL (BMI·NTF_2) forming supramolecular ionic species. The

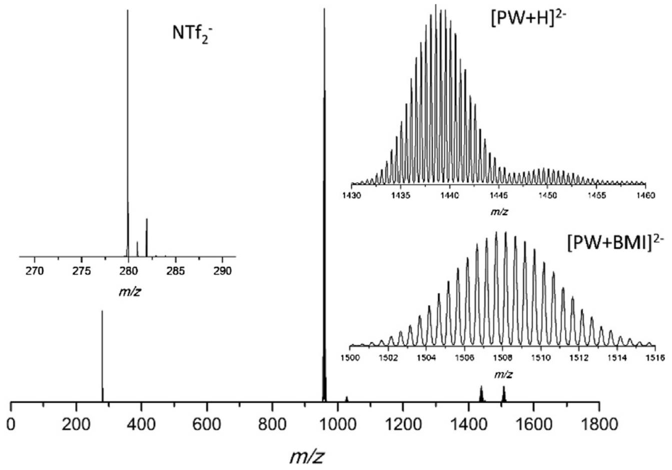

Fig. 3. ESI(−)-MS of the methanolic solution of the **MSI$_3$PW** catalyst in the presence of BMI·NTf$_2$. BMI is 1-*n*-buthyl-3-methyl imidazolium cation derivative (*m*/*z* 139), **PW** is $[PW_{12}O_{40}]^{3-}$ and NTf_2^- (see the inset) is the bis(trifluoromethane)sulfonamide anion (*m*/*z* 280).

reaction mixture of aniline, benzaldehyde, and acetophenone, in the presence of BMI·NTF$_2$ and **MSI$_3$PW** was therefore monitored (Fig. 4).

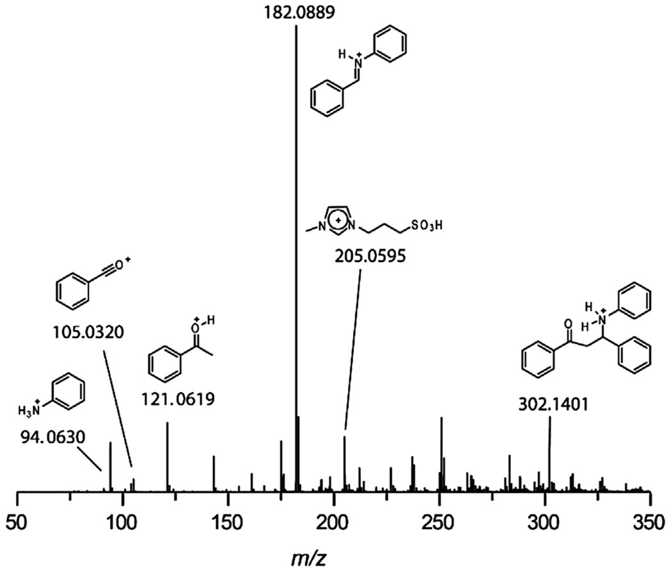

Fig. 4. ESI(+)-MS of the Mannich reaction solution catalyzed by **MSI$_3$PW** in the presence of BMI·NTf$_2$.

Fortunately, several cationic intermediates and supramolecular cations with NTf_2^- association could be detected and properly characterized by ESI(+)-MS/MS. Importantly, before the iminium ion formation (the first step of the mechanism of the Mannich reaction) no other intermediate (or the Mannich adduct) associated with this MCR could be detected. This result indicates that the limiting step of the reaction is indeed the formation of the iminium ion, which could be detected only after an overnight monitoring at 30 °C. A pre-formed iminium ion (a white solid formed upon heating pure aniline with pure benzaldehyde) was also used with similar results. Before the appearance of the iminium ion of *m*/*z* 182, only the protonated aniline (*m*/*z* 94), the protonated acetophenone (*m*/*z* 121), the **MSI** cation (*m*/*z* 205), and the BMI cation (*m*/*z* 139) could be detected. After its appearance, however, the protonated Mannich adduct of *m*/*z* 302 was detected and subjected to ESI(+)-MS/MS (Fig. 5).

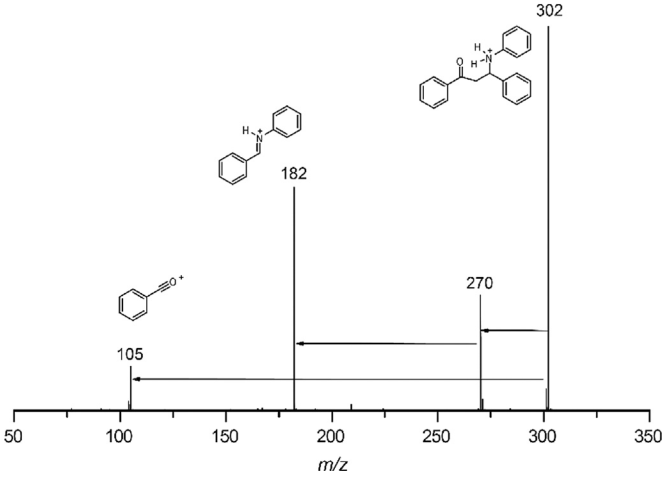

Fig. 5. ESI(+)-MS/MS of the Mannich adduct of *m*/*z* 302.

Two important supramolecular ions of *m*/*z* 644 and *m*/*z* 601 were also detected and characterized by ESI(+)-MS/MS (Figs. 6 and 7). This result demonstrates the intervention of the IL components in the formation and stabilization of the charged intermediates of the Mannich reaction.

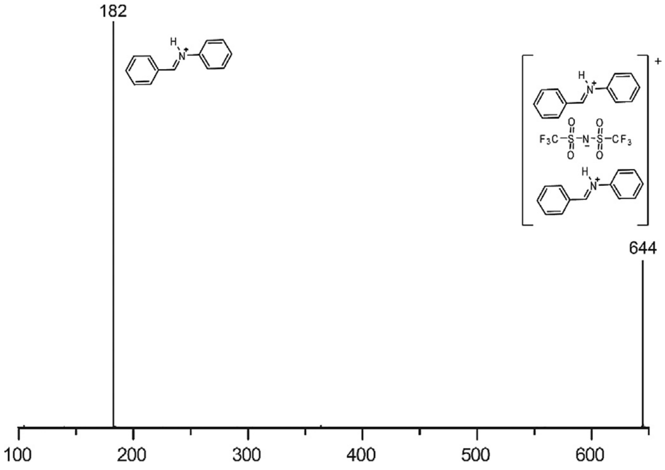

Fig. 6. ESI(+)-MS/MS of the supramolecular ion of *m*/*z* 644.

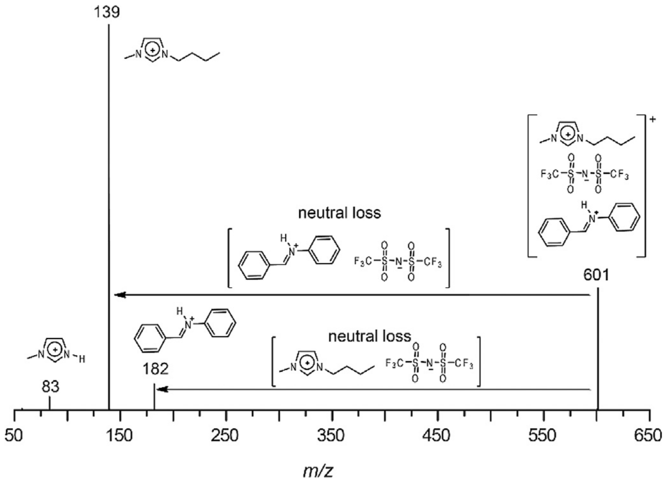

Fig. 7. ESI(+)-MS/MS of the supramolecular ion of *m*/*z* 601. Note the neutral loss of [iminium·NTf$_2$] is favored when compared with the neutral loss of BMI·NTf$_2$.

In the supramolecular ion of *m*/*z* 644, the NTf_2^- anion (*m*/*z* 280) was found associated with two iminium cations (of *m*/*z* 182), whereas in the supramolecular ion of *m*/*z* 601, the NTf_2^- is associated with both an iminium ion (of *m*/*z* 182) and a BMI cation (of *m*/*z* 139). Note that all ESI-MS were carried out from methanolic solutions, and that this polar and protic solvent favors the dissociation of those supramolecular species, in accordance with previous results.[72] Likely therefore, the high stability of the two supramolecular aggregates of *m*/*z* 644 and *m*/*z* 601 allowed their detection and characterization by ESI(+)-MS/MS (Figs. 6 and 7) despite the methanolic solutions.

The supramolecular aggregate characterized in Fig. 6 shows that indeed ion-pairing is a key factor in the reaction solution media. This stabilizing effect of the IL cations and anions, favoring the formation and stabilization of charged (or polar) intermediates (or transition states) via both ion-pairing and larger supramolecular aggregates, is known as the IL effect.[16,17] As recently reviewed,[73] ESI-MS has been an excellent tool to detect and characterize these IL supramolecular aggregates. The detection of aggregates of the NTf_2^- anion with the key iminium ion intermediate therefore points firmly to a positive IL effect over the Mannich reaction.

Other key supramolecular aggregate of *m*/*z* 601 (Fig. 7), corresponding to the ion pair $BMI\cdot NTf_2$ associated with the key iminium ion intermediate, could also be properly intercepted and characterized. Note the loss of the neutral ion pair [iminium ion$\cdot NTf_2$] that affords BMI cation of *m*/*z* 139, as well as the loss of $BMI\cdot NTf_2$ that affords the iminium ion of *m*/*z* 182. The preferential neutral loss of [iminium ion$\cdot NTf_2$] revealed that the intrinsic relative strength of coordination is [iminium ion$\cdot NTf_2$]>$BMI\cdot NTf_2$.

Based on the data obtained by ESI-MS(/MS) and the importance of the IL effect for the Mannich reaction, a catalytic cycle proposition could be formulated including the ion-pairing effect (Scheme 3). Note that larger IL supramolecular aggregates may also take place.

The equilibrium between $BMI\cdot NTf_2$ and **MSI_3PW** revealed by ESI-MS monitoring shows that the **MSI** cation is extensively or totally replaced by the BMI cation in associations with the **PW^{3-}** anion (Scheme 3). NTf_2^- is known to be an anion of very low coordination strength[74] therefore the cation **MSI** is more available and likely therefore the acidic hydrogen dissociation occurs at a larger extension. The aldehyde is then protonated and the amine addition, affording the key iminium intermediate, takes place. The iminium ion, as a charged intermediate, is capable of forming ion

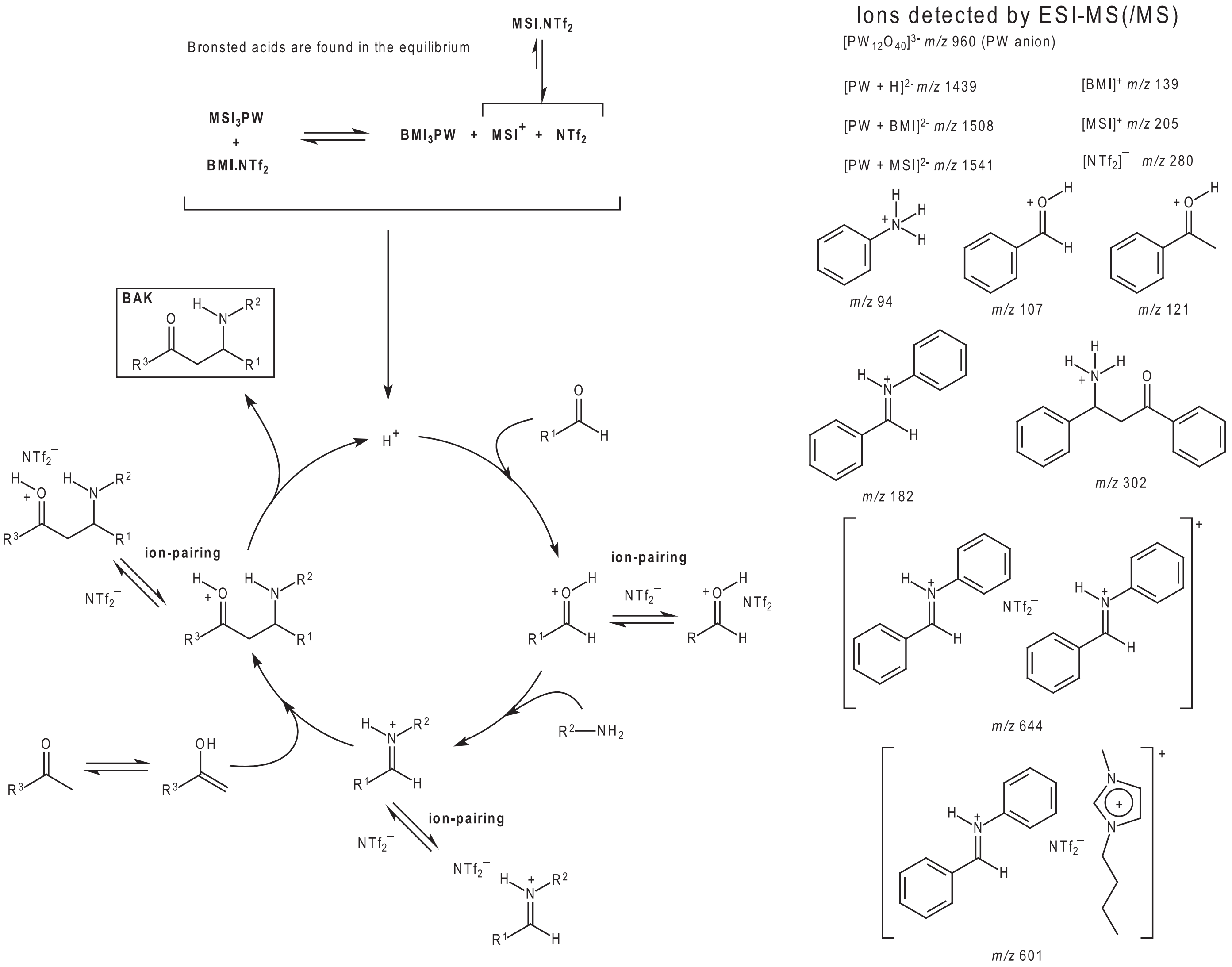

Scheme 3. Mannich three-component catalytic cycle with ionic liquid effect (left). Note the equilibrium between **MSI_3PW** and $BMI\cdot NTf_2$ revealed by ESI-MS monitoring. The charged cationic intermediates (e.g., iminium ion) from the Mannich reaction can afford supramolecular aggregates (and ion pairs) with NTf_2^- anion. Most of the structures shown in the catalytic cycle were detected and characterized by ESI-MS(/MS) (right).

pairs with NTf_2^- anion (as noted by the MS experiments) and also to associate affording larger supramolecular aggregates. Upon aggregation, additional stabilizing effects are expected. Finally, the addition to the iminium ion takes place followed by product release and restoration of the acidic catalyst.

In order to gain insight as to the importance of the IL effect in the stabilization of the charged intermediates in the Mannich MCR, theoretical calculations (DFT) were also performed. The DFT investigations were centered on the key supramolecular intermediate of *m*/*z* 601 (Fig. 7) intercepted and characterized by ESI-MS(/MS). All structures had their geometries fully optimized at B3LYP/6-31+G(d,p) level of theory and single point performed at M062X/6-311++G(2d,2p) level of calculations. After optimization, the thermodynamics properties for the dissociations of the two observed ion pairs (neutral loss) i.e. via [iminium ion·NTf_2] or BMI·NTf_2 loss from the supramolecular ion of *m*/*z* 601 (Fig. 8) were calculated.

The threshold energy (ΔH) required to dissociate the iminium ion intermediate from the supramolecular structure (i.e., neutral loss of BMI·NTf_2) is considerably higher than that to remove the imidazolium ion (i.e., neutral loss of [iminium ion·NTf_2]), therefore in accordance with the results obtained from the ESI-MS/MS experiments (Fig. 7).

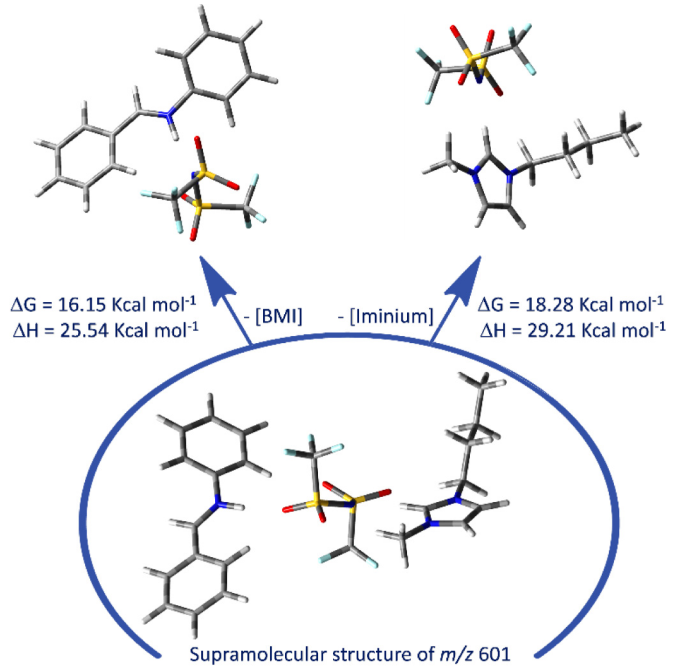

Fig. 8. Thermodynamic for the two observed ion pairs dissociations from the supramolecular ion of *m*/*z* 601. (Left) Neutral loss of [iminium ion·NTf_2]. (Right) Neutral loss of BMI·NTf_2. Calculations at M062X/6-311++G(2d,2p)//B3LYP/6-31+G(d,p) level of theory.

Finally, we calculated the IL effect via the formation of a supramolecular aggregate of two ion pairs, i.e., {[iminium ion·NTf_2]+[BMI·NTf_2]} (Fig. 9), which was found to be associated with a ΔG of $-2.53\,\mathrm{Kcal\,mol^{-1}}$ ($\Delta H = -12.01\,\mathrm{Kcal\,mol^{-1}}$; $\Delta S = -31.79\,\mathrm{cal\,mol^{-1}\,K^{-1}}$) hence spontaneous and energetically favored.

In summary, we have demonstrated that the TSIL **MSI$_3$PW** functions as a very efficient catalyst for the Hantzsch and Mannich MCR to obtain bioactive compounds in excellent yields. ESI-MS(/MS) investigations allowed a better comprehension on the intervention of supramolecular species on the mechanism of the Mannich MCR with the IL components. By ESI-MS(/MS) it was possible to detect and characterize key supramolecular aggregates pointing to the positive effect of the IL over the Mannich reaction in the formation and stabilization of charged intermediates, particularly the key iminium ion intermediate. DFT calculations showed how pronounced is the IL effect to facilitate the formation and stabilization of the this key intermediate (rate-limiting step) as well as the other charged intermediates trough both ion-pairing and the formation of larger supramolecular aggregates.

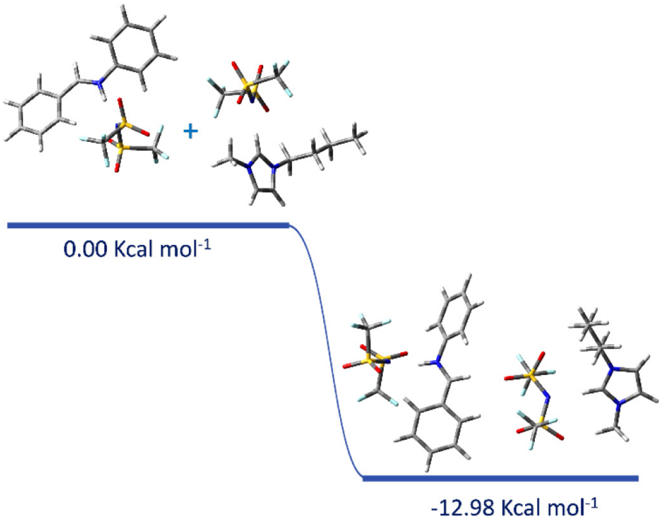

Fig. 9. Relative energy profile for the formation of the supramolecular aggregate {[iminium ion·NTf_2]+[BMI·NTf_2]} at the M062X/6-311++G(2d,2p)//B3LYP/6-31+G(d,p) level of calculation.

3. Experimental section

3.1. General

Chemicals and solvents were purchased from commercial sources. Liquid reagents and solvents were distilled prior to be used. ESI-MS and ESI-MS/MS measurements were performed in the positive ion mode (*m*/*z* 50–2000 range) on an HDMS instrument. This instrument has a hybrid quadrupole/ion mobility/orthogonal acceleration time-of-flight (oa-TOF) geometry and was used in the TOF V+ mode. All samples were dissolved in methanol to form 100 μM solutions and were directly infused into the ESI source at a flow rate of 15 μL/min after 18 h at 30 °C. ESI source conditions were as follows: capillary voltage 3.0 kV, sample cone 20 V, extraction cone 3 V. NMR spectra were recorded on a 7.05 T instrument using a 5-mm internal diameter probe operating at 300 MHz for ^1H and at 75 MHz for ^{13}C. Chemical shifts were expressed in parts per million (ppm) and referenced by the signals of the residual hydrogen atoms of the deuterated solvent ($CDCl_3$ or DMSO-d_6), as indicated in the legends. All electronic structure calculation performed in this work were performed within Kohn–Sham Density Functional Theory (DFT) formalism.[75,76] The geometry optimizations were carried out using the B3LYP/6-31+G(d,p) level of calculation. At the same level of theory, the fundamental vibrational frequency calculations were carried out to ensure the true minima, to compute zero-point vibrational energy (ZPVE) and to derive the thermochemical corrections for the heat of formation, Gibbs free energy, and the binding energy. The calculated frequencies were scaled by a factor of 0.9642 and the ZPVE and thermodynamic functions were calculated at 298.15 K and 1 atm. The optimized geometries were used for the single point calculation at M062X/6-311++g(2d,2p) level of calculation. The M062X meta exchange-correlation functional is recommend for applications involving main-group thermochemistry, kinetics, noncovalent interactions, and electronic excitation energies to valence and Rydberg states.[77] To avoid a basis-set superposition error (BSSE) the thermodynamics properties and bind energies were counter-poise corrected using a standard approach by Boys and Bernardi.[78] All theoretical calculations were carried out using Gaussian 09 program suite.[79]

The known **MSI** cation[80] was synthesized as it follows: to a solution of 1,3-propanesultone (20 mmol) dissolved in toluene (100 mL) is added 1-methylimidazole (20 mmol). The solution is allowed to react at 100 °C for 24 h and the white zwitterionic solid formed is washed with ethyl acetate, filtrated, and dried in vacuum. The known **MSI$_3$PW**[42] is prepared by treating the zwitterionic solid (15 mmol) with HPW (5 mmol) in 30 mL of water/methanol (1:1) at 50 °C for 24 h. After, the solvent is concentrated under vacuum and a white solid precipitates. The solid is washed with ethyl ether and dried in vacuum affording the desired product in quantitative yield.

3.2. General procedure for the Hantzsch reaction

A sealed Schlenk tube containing 0.5 mL of $BMI\cdot NTf_2$, 1.00 mmol of the aldehyde, 2.00 mmol of the 1,3-dicarbonyl compound, 1.00 of NH_4OAc, and **MSI$_3$PW** (5 mol %) was allowed to react at 90 °C for 4 h. Substrates were purified by chromatographic column eluted with mixtures of hexane/ethyl acetate or, whether the product precipitates in the reaction medium, it is filtered and washed with cold ethanol.

3.3. General procedure for the Hantzsch reaction

A sealed Schlenk tube containing 0.5 mL of $BMI\cdot NTf_2$, 1.00 mmol of the aldehyde, 1.00 mmol of the amine, and 1.00 mmol of the ketone and **MSI$_3$PW** (5 mol %) was allowed to react at 30 °C for 20 h. Substrates were purified by chromatographic column eluted with mixtures of hexane/ethyl acetate.

*3.3.1. 1,4-Dihydro-2,6-dimethyl-4-phenyl-3,5-diethyl-ester-3,5-pyridinedicarboxylic acid—**DHP(a)**.* ^{1}H NMR (300 MHz DMSO-d_6 and δ in ppm) 1.30 (6H, t, J 7.0 Hz, OCH$_2$*Me*), 2.24 (6H, s, Me), 3.96 (2H, q, J 7.0 Hz, OC*H*$_2$Me), 3.98 (2H, q, J 7.0 Hz, OC*H*$_2$Me), 4.84 (1H, s, CH), 7.20–7.06 (5H, m, Ph) and 8.79 (1H, s, NH). ^{13}C NMR (75 MHz, DMSO-d_6) 167.4, 148.6, 147.8, 128.2, 127.8, 126.3, 102.3, 59.4, 18.7, 14.6, and 7.2.

*3.3.2. 1,4-Dihydro-4-(3-hydroxyphenyl)-2,6-dimethyl-,3,5-diethyl ester-3,5-pyridinedicarboxylic acid—**DHP(b)**.* ^{1}H NMR (300 MHz DMSO-d_6 and δ in ppm) 2.23 (6H, t, J 7.0 Hz, OCH$_2$*Me*), 2.50 (6H, s, Me), 3.98 (4H, q, J 7 Hz, OC*H*$_2$Me), 4.00 (4H, q, J 7 Hz, OC*H*$_2$Me), 4.81 (1H, s, CH), 7.11–6.94 (5H, m, Ph), 8.77 (1H, s, OH) and 9.37 (1H, s, NH). ^{13}C NMR (75 MHz, DMSO-d_6) 167.5, 157.4, 149.8, 145.6, 129.1, 129.0, 128.5, 108.3, 102.2, 59.4, 18.7, 14.6, and 7.2.

*3.3.3. 1,4-Dihydro-2,6-dimethyl-,3,5-diethyl ester,3,5-pyridinedicarboxylic acid—**DHP(c)**.* ^{1}H NMR (300 MHz DMSO-d_6 and δ in ppm) 1.16 (6H, t, J 7.0 Hz, OCH$_2$*Me*), 2.08 (6H, s, Me), 3.33 (1H, s, CH$_a$*H*$_b$), 3.05 (1H, s, C*H*$_a$H$_b$), 4.03 (4H, q, J 7.0 Hz, OC*H*$_2$Me) and 8.25 (1H, s, NH). ^{13}C NMR (75 MHz, DMSO-d_6) 167.5, 146.9, 97.4, 59.3, 18.4, 14.8, and 7.2.

*3.3.4. 9-(1,3-Benzodioxol-5-yl)-3,4,6,7,9,10-hexahydro-1,8(2H,5H)-acridinedione—**DHP(d)**.* ^{1}H NMR (300 MHz $CDCl_3$ and δ in ppm) 2.00 (4H, m, C*H*$_2$CH$_2$CH$_2$), 2.31 (4H, m, CH$_2$C*H*$_2$CH$_2$), 2.60 (4H, m, CH$_2$CH$_2$C*H*$_2$), 4.72 (1H, s, CH), 5.8 (2H, s, OCH$_2$O) and 6.66–6.78 (3H, m, Ph), 7.26 (1H, s, NH). ^{13}C NMR (75 MHz, $CDCl_3$) 195.7, 166.9, 149.3, 148.2, 134.8, 128.6, 122.8, 121.3, 111.1, 104.9, 60.1, 50.6, 40.8, 36.9, 32.7, 29.4, 27.0, 19.4, 14.1, and 11.9.

*3.3.5. 3,4,6,7,9,10-Hexahydro-3,3,6,6-tetramethyl-9-phenyl-1,8(2H,5H)-acridinedione—**DHP(e)**.* ^{1}H NMR (300 MHz DMSO-d_6 and δ in ppm) 1.01 (12H, s, Me), 2.07 (4H, s, CH$_2$), 2.30 (4H, s, CH$_2$CO), 4.26 (1H, s, CH), 5.93 (1H, s, NH) e 7.47–6.92 (5H, m, Ph). ^{13}C NMR (75 MHz, DMSO-d_6) 206.4, 196.5, 187.7, 163.3, 141.5, 128.3, 126.8, 114.8, 47.0, 31.8, and 28.2.

*3.3.6. 3-Diphenyl-3-(phenylamino)-1-propanone—**BAK(a)**.* ^{1}H NMR (300 MHz $CDCl_3$ and δ in ppm) 3.41(1H, dd, J 16.0, 7.3 Hz, C*H*$_a$H$_b$), 3.51 (1H, dd, J 16.0, 5.5 Hz, CH$_a$*H*$_b$), 5.00 (1H, dd, J 7.3, 5.5 Hz, CH), 6.56 (2H, m, Ph), 6.65 (1H, m, Ph), 7.23 (1H, m, Ph), 7.31 (2H, t, J 7.5 Hz, Ph), 7.47–7.42 (2H, m, Ph), 7.46 (4H, m, Ph), 7.56 (1H, t, J 7.5 Hz, Ph), 7.91 (2H, d, J 6.0 Hz, Ph). ^{13}C NMR (75 MHz, $CDCl_3$) 198.7, 146.9, 142.9, 136.6, 133.4, 129.1, 128.8, 128.2, 126.3, 117.7, 113.8, 54.7, 46.3.

*3.3.7. 3-[(4-Aminophenyl)amino]-1,3-diphenylpropan-1-one—**BAK(b)**.* ^{1}H NMR (300 MHz $CDCl_3$ and δ in ppm): 3.50 (d, J 6.0 Hz, CH$_2$), 5.03 (q, J 6.0 Hz, CH), 6.60 (m, Ph), 7.11 (m, Ph), 7.19–7.62 (m, Ph), 7.80–7.95 (m, Ph). ^{13}C NMR (75 MHz, $CDCl_3$): 196.6, 189.7, 141.6, 133.3, 130.6, 129.3, 128.8, 128.6, 124.7, 124.6, 122.4, 118.8, 113.8, 54.0, and 45.8. This compound was very unstable.

*3.3.8. 3-[(4-Nitrophenyl)amino]-1,3-diphenyl-1-propanone—**BAK(c)**.* ^{1}H NMR (300 MHz $CDCl_3$ and δ in ppm) 3.52 (2H, d, J 6.0 Hz, C*H*$_2$), 5.10 (1H, q, J 6.0 Hz, C*H*), 5.56 (1H, d, J 6.0 Hz, NH), 6.51 (2H, m, Ph), 7.26–7.62 (8H, m, Ph), 7.88 (2H, m, Ph), 8.00 (2H, m, Ph). ^{13}C NMR (75 MHz, $CDCl_3$) 196.6, 189.7, 141.6, 133.3, 130.6, 129.3, 128.8, 128.6, 124.7, 124.6, 122.4, 118.8, 113.8, 54.0, and 45.8.

*3.3.9. 3-[(4-Aminophenyl)amino]-1-(4-hydroxyphenyl)-3-phenylpropan-1-one—**BAK(d)**.* ^{1}H NMR (300 MHz DMSO-d_6 and δ in ppm): 3.41 (CH$_2$), 5.02 (CH), 5.20 (NH), 6.61 (Ph), 6.85 (Ph), 7.07–8.01 (Ph). ^{13}C NMR (75 MHz, DMSO-d_6): 162.0, 160.1, 154.1, 149.2, 147.9, 143.9, 139.3, 136.7, 136.6, 136.4, 136.0, 131.3, 130.5, 130.2, 128.7, 128.6, 127.8, 126.6, 123.5, 122.4, 122.2, 122.1, 121.9, 114.2, and 30.6. This compound was very unstable.

*3.3.10. 3-(1,3-Benzodioxol-5-yl)-3-[(4-nitrophenyl)amino]-1-phenyl-1-propanone—**BAK(e)**.* ^{1}H NMR (300 MHz DMSO-d_6 and δ in ppm): 3.76 (CH$_2$), 5.17 (CH), 6.61 (Ph), 7.24 (Ph), 7.35 (Ph), 7.44–8.02 (Ph). ^{13}C NMR (75 MHz, DMSO-d_6): 196.5, 153.5, 142.5, 136.4, 135.8, 133.3, 128.6, 128.5, 128.0, 127.1, 126.5, 125.9, 52.2, 45.8, and 30.6. This compound was very unstable.

Acknowledgements

This work has been supported in part by CAPES, CNPq, FINEP-MCT, FINATEC, FAPESP, FAPDF, DPP-UnB, INCT-Catalysis, INMETRO, and ANP-PETROBRAS. DADN thanks Roberto F. de Souza for the fruitful discussions regarding the IL effect.

Supplementary data

NMR spectra, Cartesian coordinates, energies and thermal corrections for all of the calculated structures are available as Supplementary data. Supplementary data related to this article can be found at http://dx.doi.org/10.1016/j.tet.2013.10.033.

References and notes

1. Brauch, S.; van Berkel, S. S.; Westermann, B. *Chem. Soc. Rev.* **2013**, *42*, 4948–4962.
2. Gupta, A. K.; Singh, N.; Singh, K. N. *Curr. Org. Chem.* **2013**, *17*, 474–490.
3. Ren, Y. M.; Cai, C.; Yang, R. C. *RSC Adv.* **2013**, *3*, 7182–7204.
4. Aleman, J.; Cabrera, S. *Chem. Soc. Rev.* **2013**, *42*, 774–793.
5. Domling, A.; Wang, W.; Wang, K. *Chem. Rev.* **2012**, *112*, 3083–3135.
6. Slobbe, P.; Ruijter, E.; Orru, R. V. A. *Med. Chem. Commun.* **2012**, *3*, 1189–1218.
7. Sheldon, R. A. *Chem. Soc. Rev.* **2012**, *41*, 1437–1451.
8. Singh, M. S.; Chowdhury, S. *RSC Adv.* **2012**, *2*, 4547–4592.
9. Syamala, M. *Org. Prep. Proced. Int.* **2009**, *41*, 1–68.
10. Gu, Y. L. *Green Chem.* **2012**, *14*, 2091–2128.
11. Climent, M. J.; Corma, A.; Iborra, S. *RSC Adv.* **2012**, *2*, 16–58.
12. Panda, S. S.; Khanna, P.; Khanna, L. *Curr. Org. Chem.* **2012**, *16*, 507–520.
13. de Graaff, C.; Ruijter, E.; Orru, R. V. A. *Chem. Soc. Rev.* **2012**, *41*, 3969–4009.
14. Toure, B. B.; Hall, D. G. *Chem. Rev.* **2009**, *109*, 4439–4486.
15. Wegner, J.; Ceylan, S.; Kirschning, A. *Adv. Synth. Catal.* **2012**, *354*, 17–57.
16. Dupont, J.; Scholten, J. D. *Chem. Soc. Rev.* **2010**, *39*, 1780–1804.
17. Dupont, J. *Acc. Chem. Res.* **2011**, *44*, 1223–1231.
18. Scholten, J. D.; Leal, B. C.; Dupont, J. *ACS Catal.* **2012**, *2*, 184–200.
19. Chauvin, Y.; Mussmann, L.; Olivier, H. *Angew. Chem., Int. Ed.* **1996**, *34*, 2698–2700.
20. Carmichael, A. J.; Earle, M. J.; Holbrey, J. D.; McCormac, P. B.; Seddon, K. R. *Org. Lett.* **1999**, *1*, 997–1000.
21. De Bellefon, C.; Pollet, E.; Grenouillet, P. *J. Mol. Catal. A: Chem.* **1999**, *145*, 121–126.
22. Hallett, J. P.; Welton, T. *Chem. Rev.* **2011**, *111*, 3508–3576.
23. Welton, T. *Chem. Rev.* **1999**, *99*, 2071–2083.
24. Welton, T. *Coord. Chem. Rev.* **2004**, *248*, 2459–2477.
25. Plechkova, N. V.; Seddon, K. R. *Chem. Soc. Rev.* **2008**, *37*, 123–150.
26. Petkovic, M.; Seddon, K. R.; Rebelo, L. P. N.; Pereira, C. S. *Chem. Soc. Rev.* **2011**, *40*, 1383–1403.
27. Isambert, N.; Duque, M. D. S.; Plaquevent, J. C.; Genisson, Y.; Rodriguez, J.; Constantieux, T. *Chem. Soc. Rev.* **2011**, *40*, 1347–1357.
28. Shanab, K.; Neudorfer, C.; Schirmer, E.; Spreitzer, H. *Curr. Org. Chem.* **2013**, *17*, 1179–1187.
29. Sharma, N.; Kumar Sharma, U.; Kumar, R.; Richa; Kumar Sinha, A. *RSC Adv.* **2012**, *2*, 10648–10651.
30. Fang, D.; Zhang, D. Z.; Liu, Z. L. *Monatsh. Chem.* **2010**, *141*, 419–423.
31. Shaabani, A.; Rahmati, A.; Naderi, S. *Bioorg. Med. Chem. Lett.* **2005**, *15*, 5553–5557.
32. Giernoth, R. *Angew. Chem., Int. Ed.* **2010**, *49*, 2834–2839.
33. Sebesta, R.; Kmentova, I.; Toma, S. *Green Chem.* **2008**, *10*, 484–496.
34. Lombardo, M.; Trombini, C. *Chem. Cat Chem.* **2010**, *2*, 135–145.
35. Lee, S. G. *Chem. Commun.* **2006**, 1049–1063.
36. Ramos, L. M.; Tobio, A.; dos Santos, M. R.; de Oliveira, H. C. B.; Gomes, A. F.; Gozzo, F. C.; de Oliveira, A. L.; Neto, B. A. D. *J. Org. Chem.* **2012**, *77*, 10184–10193.
37. Ramos, L. M.; Guido, B. C.; Nobrega, C. C.; Corrêa, J. R.; Silva, R. G.; de Oliveira, H. C. B.; Gomes, A. F.; Gozzo, F. C.; Neto, B. A. D. *Chem.—Eur. J.* **2013**, *19*, 4156–4168.
38. Alvim, H. G. O.; de Lima, T. B.; de Oliveira, H. C. B.; Gozzo, F. C.; de Macedo, J. L.; Abdelnur, P. V.; Silva, W. A.; Neto, B. A. D. *ACS Catal.* **2013**, *3*, 1420–1430.
39. dos Santos, M. R.; Gomes, A. F.; Gozzo, F. C.; Suarez, P. A. Z.; Neto, B. A. D. *ChemSusChem* **2012**, *5*, 2383–2389.
40. dos Santos, M. R.; Diniz, J. R.; Arouca, A. M.; Gomes, A. F.; Gozzo, F. C.; Tamborim, S. M.; Parize, A. L.; Suarez, P. A. Z.; Neto, B. A. D. *ChemSusChem* **2012**, *5*, 716–726.
41. Oliveira, F. F. D.; dos Santos, M. R.; Lalli, P. M.; Schmidt, E. M.; Bakuzis, P.; Lapis, A. A. M.; Monteiro, A. L.; Eberlin, M. N.; Neto, B. A. D. *J. Org. Chem.* **2011**, *76*, 10140–10147.
42. Zhu, W. S.; Huang, W. L.; Li, H. M.; Zhang, M.; Jiang, W.; Chen, G. Y.; Han, C. R. *Fuel Process. Technol.* **2011**, *92*, 1842–1848.
43. Shagun, V. A.; Medvedeva, A. S.; Mareev, A. V. *Tetrahedron* **2013**, *69*, 2357–2368.
44. Liu, Y. P.; Liu, J. M.; Wang, X.; Cheng, T. M.; Li, R. T. *Tetrahedron* **2013**, *69*, 5242–5247.
45. Cekavicus, B.; Vigante, B.; Rucins, M.; Birkmane, K.; Petrova, M.; Belyakov, S.; Zuka, L.; Plotniece, A.; Pajuste, K.; Gosteva, M.; Sobolev, A. *Tetrahedron* **2013**, *69*, 5550–5557.
46. Shen, L.; Cao, S.; Wu, J. J.; Zhang, J.; Li, H.; Liu, N. J.; Qian, X. H. *Green Chem.* **2009**, *11*, 1414–1420.
47. Murthy, Y. L. N.; Rajack, A.; Ramji, M. T.; Babu, J. J.; Praveen, C.; Lakshmi, K. A. *Bioorg. Med. Chem. Lett.* **2012**, *22*, 6016–6023.
48. Montes-Avila, J.; Delgado-Vargas, F.; Diaz-Camacho, S. P.; Rivero, I. A. *RSC Adv.* **2012**, *2*, 1827–1834.
49. Kumar, R. S.; Idhayadhulla, A.; Nasser, A. J. A.; Selvin, J. *Eur. J. Med. Chem.* **2011**, *46*, 804–810.
50. Wynands, L.; Delacroix, S.; Nhien, A. N. V.; Soriano, E.; Marco-Contelles, J.; Postel, D. *Tetrahedron* **2013**, *69*, 4899–4907.
51. Szatmari, I.; Fulop, F. *Tetrahedron* **2013**, *69*, 1255–1278.
52. Chen, F. L.; Lei, M.; Hu, L. H. *Tetrahedron* **2013**, *69*, 2954–2960.
53. Eftekhari-Sis, B.; Abdollahifar, A.; Hashemi, M. M.; Zirak, M. *Eur. J. Org. Chem.* **2006**, 5152–5157.
54. Wang, R.; Li, B.-g.; Huang, T.-k.; Shi, L.; Lu, X.-x. *Tetrahedron Lett.* **2007**, *48*, 2071–2073.
55. Gong, K.; Fang, D.; Wang, H.-L.; Liu, Z.-L. *Monatsh. Chem.* **2007**, *138*, 1195–1198.
56. Arya, K.; Rajesh, U. C.; Rawat, D. S. *Green Chem.* **2012**, *14*, 3344–3351.
57. D'Oca, M. G. M.; Moraes, L. A. B.; Pilli, R. A.; Eberlin, M. N. *J. Org. Chem.* **2001**, *66*, 3854–3864.
58. Tomazela, D. M.; Moraes, L. A. B.; Pilli, R. A.; Eberlin, M. N.; D'Oca, M. G. M. *J. Org. Chem.* **2002**, *67*, 4652–4658.
59. Pilli, R. A.; Russowsky, D. *J. Org. Chem.* **1996**, *61*, 3187–3190.
60. Russowsky, D.; Petersen, R. Z.; Godoi, M. N.; Pilli, R. A. *Tetrahedron Lett.* **2000**, *41*, 9939–9942.
61. Speckamp, W. N.; Moolenaar, M. J. *Tetrahedron* **2000**, *56*, 3817–3856.
62. Coelho, F.; Eberlin, M. N. *Angew. Chem., Int. Ed.* **2011**, *50*, 5261–5263.
63. Santos, L. S. *J. Braz. Chem. Soc.* **2011**, *22*, 1827–1840.
64. Orth, E. S.; Brandao, T. A. S.; Souza, B. S.; Pliego, J. R.; Vaz, B. G.; Eberlin, M. N.; Kirby, A. J.; Nome, F. *J. Am. Chem. Soc.* **2010**, *132*, 8513–8523.
65. Amarante, G. W.; Benassi, M.; Pascoal, R. N.; Eberlin, M. N.; Coelho, F. *Tetrahedron* **2010**, *66*, 4370–4376.
66. Santos, L. S. *Eur. J. Org. Chem.* **2008**, 235–253.
67. Corilo, Y. E.; Nachtigall, F. M.; Abdelnur, P. V.; Ebeling, G.; Dupont, J.; Eberlin, M. N. *RSC Adv.* **2011**, *1*, 73–78.
68. Machado, A. H. L.; Milagre, H. M. S.; Eberlin, L. S.; Sabino, A. A.; Correia, C. R. D.; Eberlin, M. N. *Org. Biomol. Chem.* **2013**, *11*, 3277–3281.
69. Gozzo, F. C.; Santos, L. S.; Augusti, R.; Consorti, C. S.; Dupont, J.; Eberlin, M. N. *Chem.—Eur. J.* **2004**, *10*, 6187–6193.
70. Chiappe, C.; Rajamani, S. *Eur. J. Org. Chem.* **2011**, 5517–5539.
71. Johnson, K. E.; Pagni, R. M.; Bartmess, J. *Monatsh. Chem.* **2007**, *138*, 1077–1101.
72. Consorti, C. S.; Suarez, P. A. Z.; de Souza, R. F.; Burrow, R. A.; Farrar, D. H.; Lough, A. J.; Loh, W.; da Silva, L. H. M.; Dupont, J. *J. Phys. Chem. B* **2005**, *109*, 4341–4349.
73. Dupont, J.; Eberlin, M. N. *Curr. Org. Chem.* **2013**, *17*, 257–272.
74. Lapis, A. A. M.; Neto, B. A. D.; Scholten, J. D.; Nachtigall, F. M.; Eberlin, M. N.; Dupont, J. *Tetrahedron Lett.* **2006**, *47*, 6775–6779.
75. Kohn, W.; Sham, L. J. *Phys. Rev. B* **1965**, *137*, A1697–A1705.
76. Hohenberg, P.; Kohn, W. *Phys. Rev. B* **1964**, *136*, B864–B871.
77. Zhao, Y.; Truhlar, D. G. *Theor. Chem. Acc.* **2008**, *120*, 215–241.
78. Boys, S. F.; Bernardi, F. *Mol. Phys.* **1970**, *19*, 553–566.
79. Frisch, M. J.; Trucks, G. W.; Schlegel, H. B.; Scuseria, G. E.; Robb, M. A.; Cheeseman, J. R.; Scalmani, G.; Barone, V.; Mennucci, B.; Petersson, G. A.; Nakatsuji, H.; Caricato, M.; Li, X.; Hratchian, H. P.; Izmaylov, A. F.; Bloino, J.; Zheng, G.; Sonnenberg, J. L.; Hada, M.; Ehara, M.; Toyota, K.; Fukuda, R.; Hasegawa, J.; Ishida, M.; Nakajima, T.; Honda, Y.; Kitao, O.; Nakai, H.; Vreven, T.; Montgomery, J. A.; Peralta, J. E.; Ogliaro, F.; Bearpark, M.; Heyd, J. J.; Brothers, E.; Kudin, K. N.; Staroverov, V. N.; Kobayashi, R.; Normand, J.; Raghavachari, K.; Rendell, A.; Burant, J. C.; Iyengar, S. S.; Tomasi, J.; Cossi, M.; Rega, N.; Millam, J. M.; Klene, M.; Knox, J. E.; Cross, J. B.; Bakken, V.; Adamo, C.; Jaramillo, J.; Gomperts, R.; Stratmann, R. E.; Yazyev, O.; Austin, A. J.; Cammi, R.; Pomelli, C.; Ochterski, J. W.; Martin, R. L.; Morokuma, K.; Zakrzewski, V. G.; Voth, G. A.; Salvador, P.; Dannenberg, J. J.; Dapprich, S.; Daniels, A. D.; Farkas; Foresman, J. B.; Ortiz, J. V.; Cioslowski, J.; Fox, D. J. Wallingford C. T., 2009.
80. Kraus, G. A.; Guney, T. *Green Chem.* **2012**, *14*, 1593–1596.